J Therm Anal Calorim (2011) 106:407–413
DOI 10.1007/s10973-011-1475-z

Characterization of poly(vinyl acetate)/sugar cane bagasse lignin blends and their photochemical degradation

M. F. Silva · E. A. G. Pineda · A. A. W. Hechenleitner · D. M. Fernandes · M. K. Lima · P. R. S. Bittencourt

CBRATEC7 Conference Special Issue

Abstract The acetone-soluble lignin fraction (ASLF) of sugar cane bagasse, from a sugar and alcohol factory residue, was obtained after extraction with formic acid and used to prepare blends with poly(vinyl acetate) (PVAc) by casting. PVAc and ASLF/PVAc blends were irradiated with ultraviolet light (Hg lamp). Blend formation and the irradiation effects were examined through thermal analysis (TG and DSC), scanning electron microscopy, and atomic force microscopy. The DSC results show PVAc glass transition temperature (T_g) shifts because of both, irradiation and ASLF incorporation. Non-irradiated pure PVAc presented a smooth surface, while after UV irradiation, light surface spots are observed. ASLF/PVAc 10/90 and 5/95 blends did not exhibit differences before and after UV irradiation, suggesting that lignin protects PVAc from photochemical degradation.

Keywords Poly(vinyl acetate) · Lignin · FTIR · SEM · TG · DSC

Introduction

Lignin is a phenolic biopolymer (showed in Fig. 1 [1]) present in the cell wall of higher plants and mainly in woody tissues. It is obtained in large quantities as by-product in the pulp and paper industry. It can also be extracted from plant residues such as sugar cane bagasse which is the most abundant waste of the Brazilian agroindustry. Depending on its origin and extraction method, lignin structure (based on phenylpropane units) presents variations in the relative content of the functional groups: methoxyl, carbonyl, carboxyl, phenolic, and aliphatic hydroxyls. Besides its major use as energy source and in leather tanning, lignin is still investigated in various applications such as dispersant [2, 3], emulsifier [4, 5], pesticide [6], antioxidant [7–9], compatibilizer [10], filler [11, 12], and others [13, 14].

Various studies of blends containing lignin and/or its derivatives have shown that the incorporation of low amounts of them to a synthetic polymer stabilized the material against photo and/or thermal oxidation [7–9, 15–18].

Based on the earlier studies of PVA-Lignin systems [17–20] in which lignin also showed stabilizing effects, in this study the authors focused on lignin incorporation to poly (vinyl acetate) (PVAc). PVAc is a thermoplastic with good adhesion to different substrates and also with good film-forming properties. It is extensively used in paints, adhesives, architectural coatings, applications in which the polymeric material is frequently exposed to sunlight. When exposed to UV light, PVAc undergoes photooxidative degradation [21] which depends on the surrounding conditions and causes alterations such as embrittlement and discoloration, decreasing its useful lifetime. The objective of this study was to obtain a stability improvement of PVAc films toward ultraviolet radiation.

Experimental

Materials

PVAc of Mw 113,000 was purchased from Aldrich. Sugar cane bagasse was obtained from a local sugar and alcohol

M. F. Silva (✉) · E. A. G. Pineda · A. A. W. Hechenleitner · D. M. Fernandes · M. K. Lima · P. R. S. Bittencourt
Departamento de Química, Universidade Estadual de Maringá, Av. Colombo 5790, Maringá, PR 87020-900, Brazil
e-mail: celafs@gmail.com

Fig. 1 Lignin structure

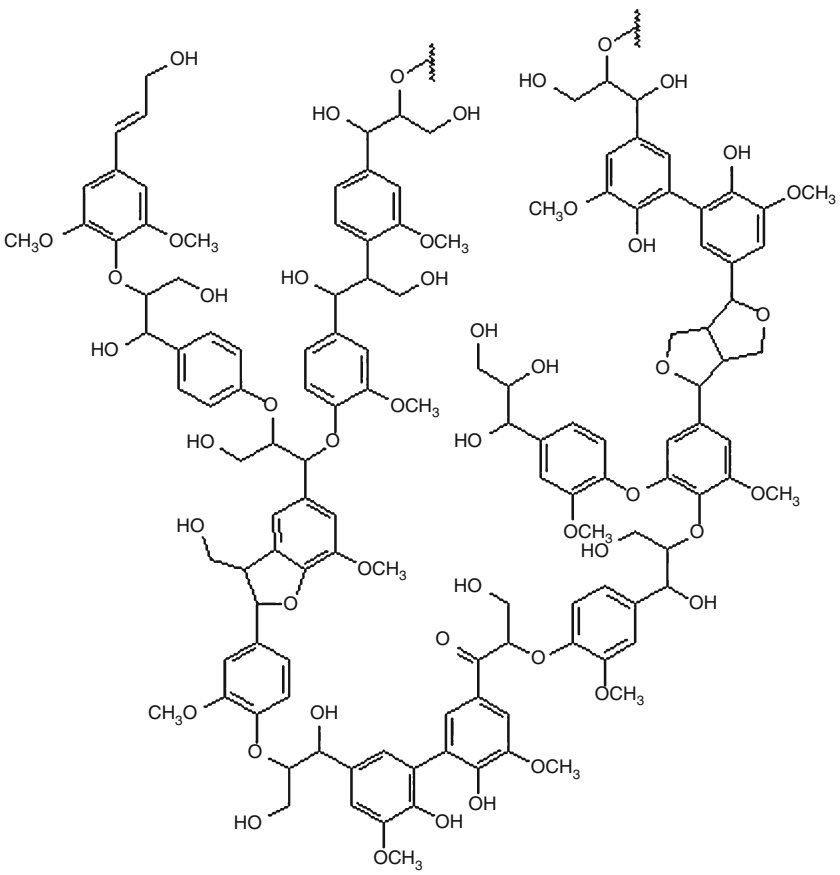

factory (Santa Terezinha, Iguatemi, PR-Brazil). Hexane, formic acid, acetone, and other used reagents were of analytical grade and purchased from Nuclear.

Methods

For lignin isolation, sugar cane bagasse was first washed with abundant water, dried, and grounded. The powder was submitted to successive extractions with *n*-hexane, ethanol, and water in a Soxhlet system to remove low-molecular weight components. The sample was then treated with an 80% FA and 1% HCl aqueous solution in the Soxhlet system in a ratio of 100 mL of solution for 10 g of sugar cane bagasse. Lignin was precipitated by diluting the dark brown solution obtained in the previous step with distilled water. After isolation by centrifugation, it was washed with water, twice redissolved in acetone for further purification, and oven dried at 60 °C. For the isolation of the acetone-soluble lignin fraction (ASLF), lignin was extracted with acetone in a Soxhlet system and then dried at 60 °C.

For blends preparation, the polymers (PVAc and ASLF) were separately dissolved in acetone (concentration of 7,2 g L^{-1}) and then mixed in appropriate amounts to give ASLF/PVAc blends with 15/85, 10/90, and 5/95 weight percent ratios. 13 mL of blend solutions mixture were stirred and transferred to poly(trifluoroethylene) (Teflon®) dishes with area of 28,3 cm^2 for solvent evaporation at 60 °C.

PVAc and ASLF/PVAc samples were irradiated for 96 h with a low-pressure Hg vapor lamp (OSRAM, 125 W) without a bulb, with 48 mJ s^{-1} m^{-2} fluence rate measured at sample surface (the distance between the lamp and the sample surface was 17 cm).

Thermogravimetric measurements were performed with a Shimadzu TGA 50 instrument in the following experimental conditions: approximately 6 mg samples, platinum pans, 10 °C min^{-1} heating rate, 20 mL min^{-1} of nitrogen flow.

DSC was performed on Shimadzu DSC-50 under flowing nitrogen (20 mL min^{-1}) atmosphere at 10 °C min^{-1}. Samples of 6 mg were placed into aluminum pans. The glass transition temperature of the samples was determined from the midpoint of the heat flux change observed in the 25–50 °C temperature range, on the second scan, at heating rate of 10 °C min^{-1}.

FTIR spectra were obtained using a FTIR BOMEM MB 100 spectrometer with samples in 1% KBr pellets.

A Shimadzu scanning electron microscope (SEM) model SS550 Superscan was used to analyze the morphology of the films coated by gold sputtering with 1000×

amplification and an area of 10 μm and a SHIMADZU SPM-9500 J3 atomic force microscope (AFM) was used to obtain images of films surface in dynamic mode.

Results and discussion

Lignin characterization

The acetone-soluble formic lignin (ASLF) obtained from sugar cane bagasse was characterized using FTIR, TGA, and DSC techniques. These results are shown in Figs. 2, 3. Characteristic absorption bands in the infrared spectrum (see Fig. 2) are: 3428 cm^{-1} (O–H stretching), 2923 and 2845 cm^{-1} (C–H stretching), 1712 cm^{-1}(C=O stretching), 1600, 1515, and 1458 cm^{-1} (aromatic ring vibrations) and other less intense peaks in the fingerprint region [22]. The intense band at 1712 cm^{-1} indicates that the lignin was formulated during pulping [23].

TG results (Fig. 3) are similar to those observed with other lignin samples [24–27], characteristic temperature of the events can show some variations and are related to the sample origin and isolation method. Mass loss because of heating in inert atmosphere doesn't presents well-defined steps, showing that the sample degradation occurs as sequence of complex reactions. Thermal degradation starts at low temperature and mass loss observed until 150 °C is attributed to evaporation of water and loss of other components with low-molar mass. From 180 °C onward, the mass loss is attributed to pyrolytic degradation that involves first the side groups of the main chain, followed by depolymerization at higher temperature, where monomeric phenols are formed. Above 500 °C the process is related to the decomposition of some aromatic rings [28]. At 1000 °C, about 5% of residual mass is observed.

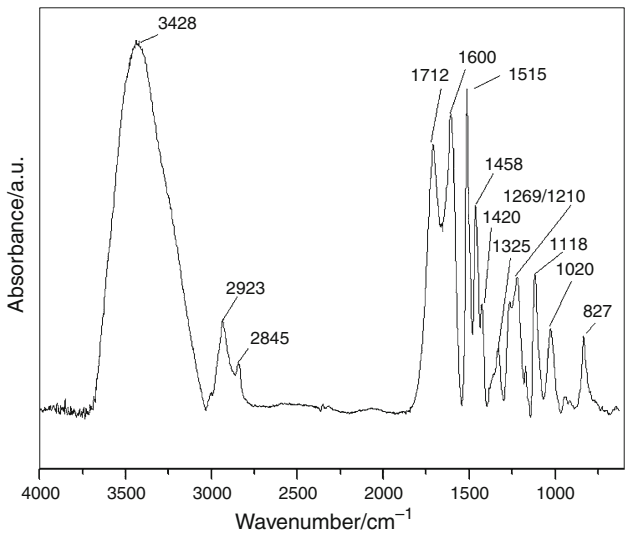

Fig. 2 FTIR spectrum of ASLF

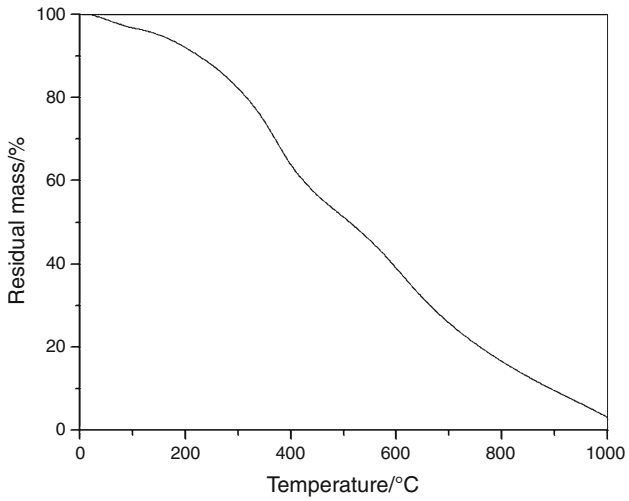

Fig. 3 Thermogravimetric curve of ASLF

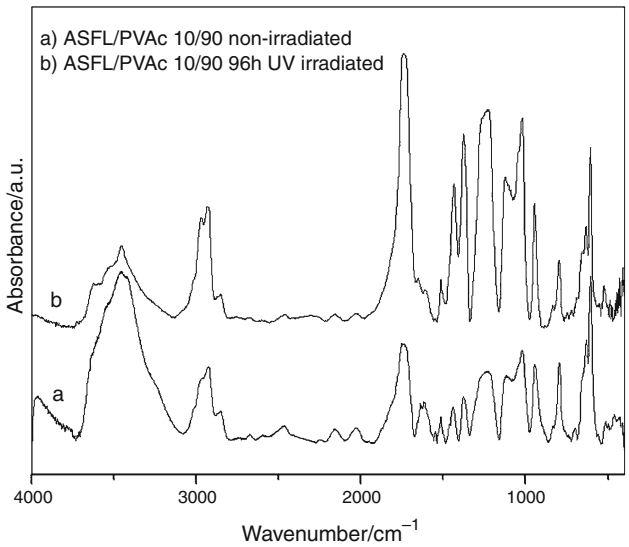

Fig. 4 FTIR spectra of the 10/90 ASFL/PVAc films non-irradiated and 96-h UV irradiated

The DSC curve for ASLF(figure not showed) present an endothermic peak because of adsorbed water evaporation near 100 °C. The glass transition for lignin samples is generally reported to occur near 100–180 °C [29–31]. It was not possible to detect the T_g of lignin undoubtedly from the DSC curves. At higher temperature, exothermic superimposed peaks can be seen which correlate with the pyrolytic degradation reactions evidenced in the TG analyses.

ASLF/PVAc blends

FTIR spectra were recorded before and after film irradiation with an Hg lamp for 96 h. The peak area ratio of the carbonyl band of the PVAc at 1740 cm^{-1} related to the

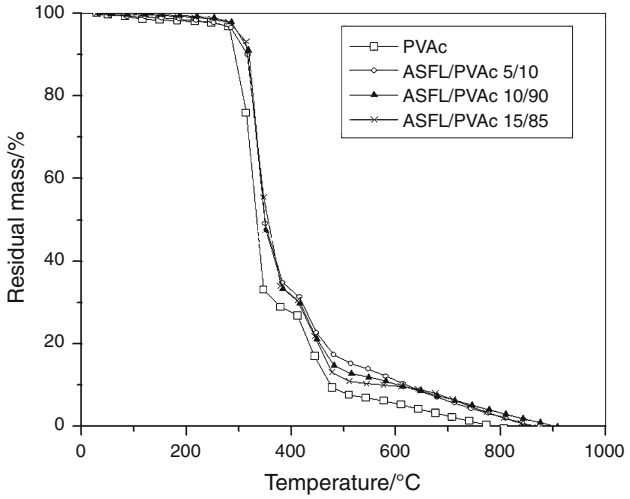

Fig. 5 Thermogravimetric curve of PVAc and ASLF/PVAc blends

total spectral area was determined for both ASFL/PVAc 10/90 samples (irradiated and non-irradiated films) and a 100% increase was observed due to the irradiation. This result shows that ultraviolet light promotes lignin structure modification. The reactions leading to products with increasing content of mentioned bond in the photo-oxidation of PVAc were described by Jin et al. [32]. UV irradiation resulted in the drastic reduction of the hydroxyl band between 3400 and 3500 cm^{-1}, due to photodegradation reactions of lignin that contains hydroxyl substituted aromatic groups that may act as hindered phenol light stabilizers. Similar results were obtained for blends 5/95 and 15/85. Figure 4 shows the loss in weight of a film of

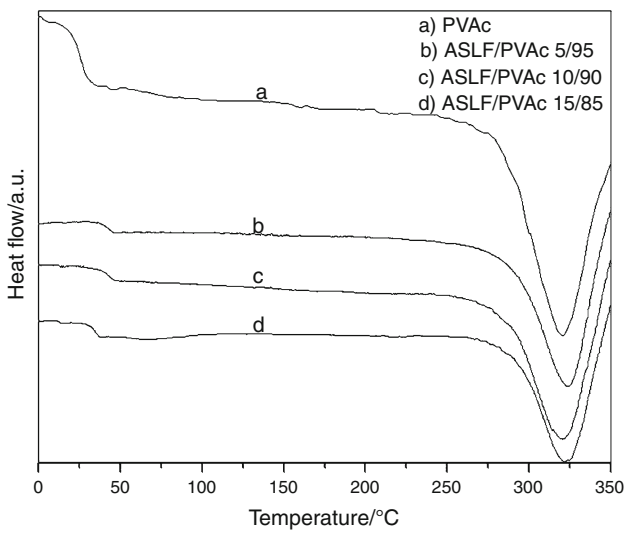

Fig. 6 DSC curve of PVAc and ASLF/PVAc blends non-irradiated

Table 1 Glass transition temperatures of PVAc and ASLF/PVAc blends

Composition (ASLF/PVAc)	T_g/°C
0/100	19
5/95	37
10/90	36
15/85	31

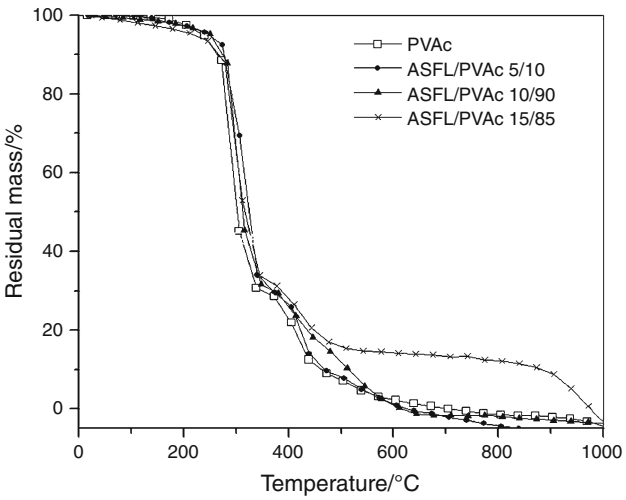

Fig. 7 Thermogravimetric curve of PVAc and ASLF/PVAc blends (96-h UV irradiated films)

Table 2 Glass transition temperatures of PVAc and ASLF/PVAc blends (irradiated films)

Composition (ASLF/PVAc)	T_g/°C
0/100	29
5/95	33
10/90	31
15/85	38

pure PVAc as well as of ASLF/PVAc blends as a function of temperature. The two main steps observed are known: (1) between 300 and 350 °C in which the deacetylation process takes place and (2) the disintegration of the polyolefinic backbone around 430 °C [33]. The onset of PVAc degradation occurs at approximately 300 °C and is slightly shifted to higher temperature when ASLF is incorporated (5–15%). This stabilization at the initial stage of the blends degradation can be explained considering that lignin molecules have radical scavenging action and so it can suppress to some extent the deacetylation reaction initiated by radical formation. Another effect of the ASLF incorporation to PVAc is observed above 500 °C, residual mass increases with lignin content. This can be related to the relatively high quantity of char formed by the lignin, as can be seen in Fig. 3.

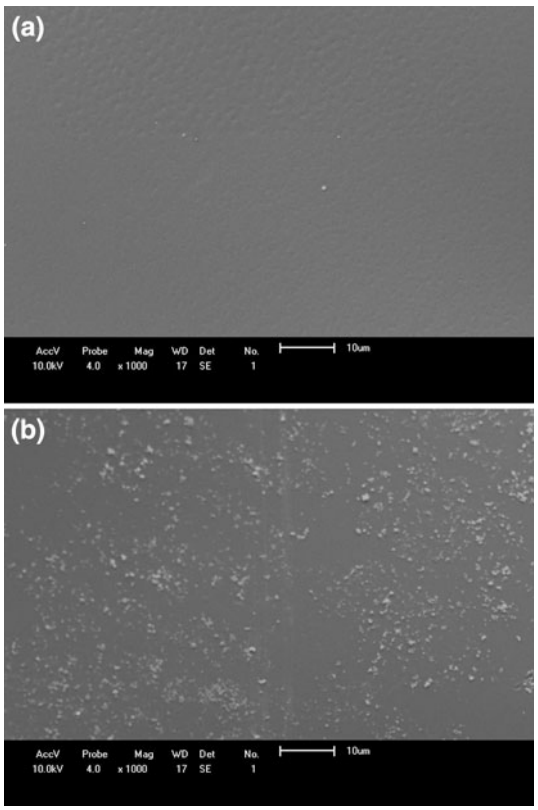

Fig. 8 SEM micrograph of the PVAc film surface **a** non-irradiated and **b** after 96-h UV

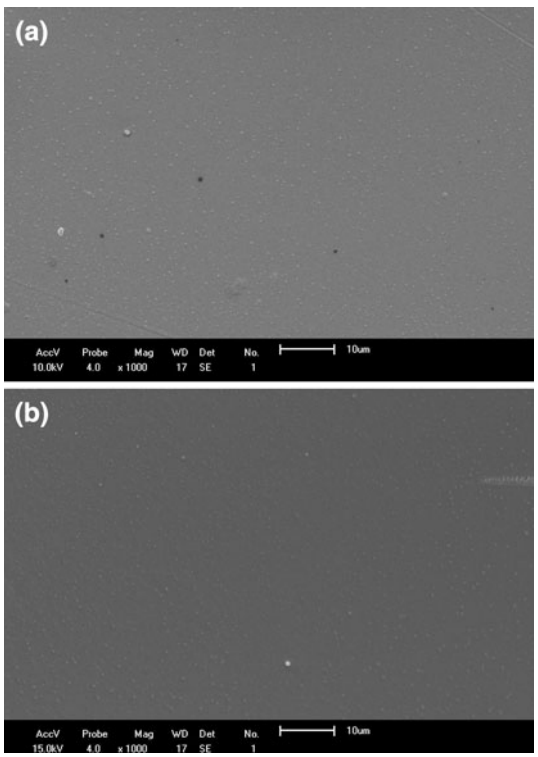

Fig. 9 SEM micrograph of the 10/90 ASLF/PVAc film **a**non-irradiated and **b** after 96-h UV irradiation

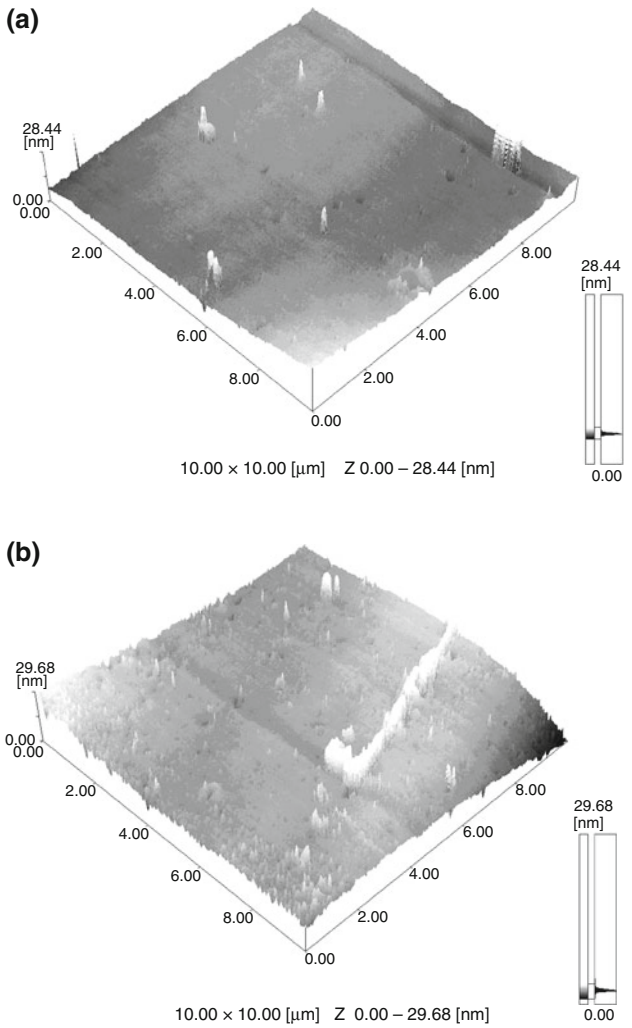

Fig. 10 AFM micrographs of surface of PVAc films **a** non-irradiated and **b** 96-h UV irradiated

DSC data (Fig. 5) of these samples showed glass transition around 20–50 °C and an endothermic degradation reaction starting at 250 °C. The T_g of PVAc increases due to lignin presence, mainly in the 5/95 and 10/90 blends, as can be seen in Table 1. This behavior is indicative of interchain interaction that can lead to some compatibility.

TG and DSC analysis of PVAc and ASLF/PVAc blends were also performed after 96 h films irradiation with UV light. TG curves (Fig. 6) are very similar with those of the nonirradiated samples (Fig. 4) showing both thermal degradation steps in practically the same temperature ranges. Nevertheless, the 10/90 and mainly the 15/85 blend show greater residual mass at temperatures above 450 °C than the corresponding non-irradiated blends, evidencing that thermal degradation reactions are different and produce higher products mass than the non-irradiated samples when they contain 10–15% of ASLF. On the other hand, DSC analysis of the irradiated films show T_g shifts due to the

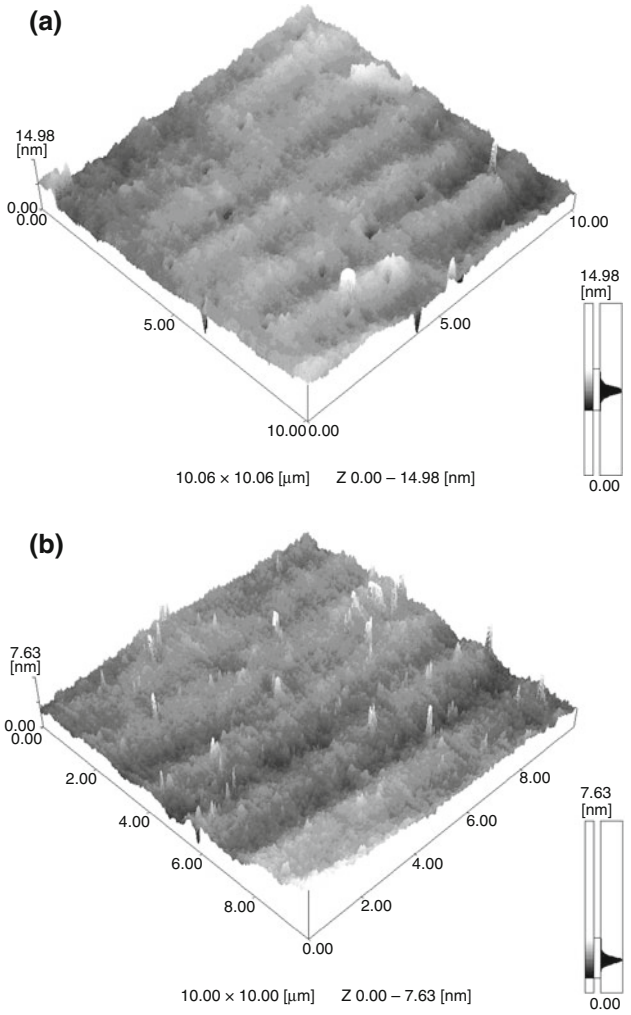

Fig. 11 AFM micrographs of ASLF/PVAc 10/90 surface films **a** non-irradiated and **b** 96-h UV irradiation

irradiation, as can be seen comparing data in Tables 1 and 2. The difference in T_g, of each irradiated and corresponding non-irradiated sample, is lower for the 5/95 and 10/90 blends compared with the pure PVAc. The 15/85 blend show a different behavior, T_g increases in a similar extent as occurs with the pure PVA. The manner in which the glass transition temperature (T_g) varies with blend composition is reflective of the relative strengths of these intermolecular interactions. Probably in this composition there is a major tendency of phase separation. Small concentration of lignin (ASFL/PVAc 5/95 and 10/90) presents more compatibility than high-concentration blends, showing that protect effect is lignin concentration dependent.

The films morphology was studied by SEM. Figures 7 and 8 show the SEM micrographs of the 0/100 and 10/90 films (before UV irradiation and after 96-h UV irradiation), respectively.

The morphology of the non-irradiated PVAc film is characterized by a smooth surface, and after irradiation, it presented a smooth surface with regular clear formations caused by photodegradation. Most probably photochemical reactions occur in the superficial layers of the film, which frequently involves C–O–C and C=O groups, that in turn can involve the splitting of the chains of the polymer.

The 10/90 ASLF/PVAc film was characterized by the presence of small globular structures homogeneously distributed, related to lignin. The presence of different phases in the structure may be indicative of the immiscibility or partial miscibility of the polymers. After 96-h UV irradiation, the film maintains the same characteristics, distinctly from the degradation evidences observed in pure PVAc. As suggested by the DSC analyses, the authors can propose interactions between the PVAc and ASLF chains, and that ASLF protects PVAc from degradation by UV irradiation. This probably occurs due to the lignin aromatic groups, which absorb UV light, forming phenoxy radicals, hindering PVAc degradation [34, 35].

AFM micrographs of non-irradiated and irradiated PVAc are shown in Fig. 9 and micrographs of non-irradiated and irradiated 10/90 films are shown in Fig. 10. As in the SEM micrographs, in these images it can be observed that for pure PVAc film, irradiation causes irregularities formation and that for the 10/90 film, irradiation effect is practically non-detectable (Fig. 11).

Conclusions

Good quality films of pure PVAc and of ASLF/PVAc blends were obtained by casting, using acetone as solvent. Polymers show compatibility in the 5/95 and 10/90 compositions evidenced by microscopic and DSC results. PVAc undergoes photodegradation under UV irradiation; however, in the presence of 10% of ASLF, this effect is reduced. Practically the same surface morphology is observed in SEM and AFM images for the ASLF/PVAc 10/90 before and after UV irradiation, while for pure PVAc significant differences are visible. These results suggest that lignin protects PVAc from photochemical degradation and that it has important potential to be used as stabilizing component in PVAc films, especially in cases were the films application includes sunlight exposure.

References

1. Gregory AP (2007) Green energy. In: Odyssey.http://www.research.uky.edu/odyssey/winter07/green_energy.html. Accessed 15 Feb 2011.
2. Zhou M, Kong Q, Pan B, Qiu X, Yang D, Lou H. Evaluation of treated black liquor used as dispersant of concentrated coal-water slurry. Fuel. 2010;89:716–23.

3. Zhao X, Liu D. Chemical and thermal characteristics of lignins isolated from Siam weed stem by acetic acid and formic acido delignification. Ind Crops Prod. 2010;32:284–91.
4. Toledano A, Mondragon AGI, Labidi J. Lignin separation and fractionation by ultrafiltration. Sep Purif Technol. 2010;71:38–43.
5. Serrano L, Egües I, Alriols MG, Llano-Ponte R, Labidi J. *Miscanthus sinensis* fractionation by different reagents. Chem Eng J. 2010;156:49–55.
6. Fernándes-Pérez M, Villafranca-Sánchez M, Flores-Céspedes F, Pérez-García S, Daza-Fernández I. Prevention of chloridazon and metribuzin pollution using lignin-based formulations. Environ Poll. 2010;158:1412–9.
7. García A, Toledano A, Andrés MA, Labidi J. Study of antioxidant capacity of *Miscanthus sinensis* lignins. Proc Biochem. 2010;45:935–40.
8. Wörmeyer B, Ingrama T, Saake B, Brunner G, Smirnova I. Comparison of different pretreatment methods for lignocellulosic materials. Part II: influence of pretreatment on the properties of rye straw lignin. Bioresour Technol. 2011;102:4157–64.
9. Sivasankarapillai G, McDonald AG. Synthesis and properties of lignin-highly branched poly(ester-amine) polymeric systems. Biomass Bionerg. 2011;35:919–31.
10. Sailaja RRN, Deepthi MV. Mechanical and thermal properties of compatibilized composites of polyethylene and esterified lignin. Mater Des. 2010;31:4369–79.
11. Doherty WOS, Mousavioun P, Fellows CM. Value-adding to cellulosic ethanol: lignin polymers. Ind Crops Prod. 2011;33:259–76.
12. Tian M, Wen J, MacDonald D, Asmussen RM, Chen A. A novel approach for lignin modification and degradation. Electrochem Commun. 2010;12:527–30.
13. Sakagami H, Kushida T, Oizumi T, Nakashima H, Makino T. Distribution of lignin–carbohydrate complex in plant kingdom and its functionality as alternative medicine. Pharmacol Ther. 2010;128:91–105.
14. Kriaa A, Hamdi N, Srasra E. Removal of Cu (II) from water pollutant with Tunisian activated lignin prepared by phosphoric acid activation. Desalination. 2010;250:179–87.
15. Mousavioun P, Doherty WOS, Georg G. Thermal stability and miscibility of poly(hydroxybutyrate) and soda lignin blends. Indl Crops and Prod. 2010;32:656–61.
16. Rosa IM, Kenny JM, Puglia D, Santulli C, Sarasini F. Morphological, thermal and mechanical characterization of okra (*Abelmoschus esculentus*) fibres as potential reinforcement in polymer composites. Comp Sci Technol. 2010;70:116–22.
17. Bittencourt PRS, Fernandes DM, Silva MF, Lima MK, Hechenleitner AAW, Pineda EAG. Lignin modified by formic acid on the PA6 films: evaluation on the morphology and degradation by UV radiation. Waste Biomass Valor. 2010;1:323–8.
18. Silva MF, da Silva CA, Fogo FC, Pineda EA, Hechenleitner AAW. Thermal and FTIR study of polyvinylpyrrolidone/lignin blends. J Therm Anal Calorim. 2005;79:367–70.
19. Bittencourt PRS, dos Santos GL, Pineda EAG, Hechenleitner AAW. Thermal stability and film irradiation effect of poly(vinylalcohol)/kraft lignin blends. J Therm Anal Calorim. 2005;79:371–4.
20. Fernandes DM, Hechenleitner AAW, Job AE, Radovanovic E, Pineda EAG. Thermal and photochemical stability of poly vinyl alcohol/modified lignin blends. Polym Degrad Stab. 2006;91:1192–201.
21. Ferreira JL, Melo MJ, Ramos AM. Poly(vinyl acetate) paints in works of art: a photochemical approach. Part 1. Polym Degrad Stab. 2010;95:453–61.
22. Chen H, Ferrari C, Angiuli M, Yao J, Raspi C, Bramanti E. Qualitative and quantitative analysis of wood samples by fourier transform infrared spectroscopy and multivariate analysis. Carbohydr Polym. 2010;82:772–8.
23. Jahan MS, Chowdhurry DAN, Islam MK. Atmospheric formic acid pulping and TCF beaching of dhaincha (*Sesbania aculeate*), kash (*Saccharum spontaneum*) and banana stem (*Musa Cavendish*). Ind Crops Prod. 2007;26:324–31.
24. Shen DK, Gu S, Luo KH, Wang SR, Fang MX. The pyrolytic degradation of wood-derived lignin from pulping process. Bioresour Technol. 2010;101:6136–46.
25. Faravelli T, Frassoldati A, Migliavacca G, Ranzi E. Detailed kinetic modeling of the thermal degradation of lignins. Biomass Bioenerg. 2010;34:290–301.
26. Ibrahima MNM, Ahmed-Haras MR, Sipaut CS, Aboul-Enein HY, Mohamed AA. Preparation and characterization of a newly water soluble lignin graft copolymer from oil palm lignocellulosic waste. Carbohydr Polym. 2010;80:1102–10.
27. Buranov AU, Ross KA, Mazza G. Isolation and characterization of lignins extracted from flax shives using pressurized aqueous ethanol. Bioresour Technol. 2010;101:7446–55.
28. Jiang G, Nowakowski DJ, Bridgwater AV. A systematic study of the kinetics of lignin pyrolysis. Thermochim Acta. 2010;498:61–6.
29. Doherty WOS, Mousavioun P, Fellows CM. Value-adding to cellulosic ethanol: lignin polymers. Ind Crops Prod. 2011;33:259–76.
30. Mousavioun P, Doherty WOS. Chemical and thermal properties of fractionated bagasse soda lignin. Ind Crops Prod. 2010;31:52–8.
31. Fernández-Pérez M, Villafranca-Sánchez M, Flores-Céspedes F, Daza-Fernández I. Ethylcellulose and lignin as bearer polymers in controlled release formulations of chloridazon. Carbohydr Polym. 2011;83:1672–9.
32. Jin J, Chen S, Zhang J. UV aging behaviour of ethylene-vinyl acetate copolymers (EVA) with different vinyl acetate contents. Polym Degrad Stab. 2010;95:725–32.
33. Forsthuber B, Grüll G. The effects of HALS in the prevention of photo-degradation of acrylic clear topcoats and wooden surfaces. Polym Degrad Stab. 2010;95:746–55.
34. Popescu CM, Spiridon I, Tibirna CM, Vasile C. A thermogravimetric study of structural changes of lime wood (Tilia cordata-Mill.) induced by exposure to simulated accelerated UV/Vis-light. J Photochem Photobiol Chem. 2011;217:207–12.
35. Pucciariello R, D'Auria M, Villani V, Giammarino G, Gorrasi G, Shulga G. Lignin/poly(ε-Caprolactone) blends with tuneable mechanical properties prepared by high energy ball-milling. J Polym Environ. 2010;18:326–34.